Intra- and inter-molecular phosphoryl migration in phosphinothiazolines; precursors to polynuclear complexes and bimetallic coordination polymers†‡

Günter Margraf, Roberto Pattacini, Abdelatif Messaoudi and Pierre Braunstein*

Received (in Cambridge, UK) 9th March 2006, Accepted 24th May 2006
First published as an Advance Article on the web 14th June 2006
DOI: 10.1039/b603495k

Two tautomers of the new phosphinoaminothiazoline $Ph_2PNHC{=}NCH_2CH_2S$ (1), obtained from the reaction of 2-amino-2-thiazoline (ATHZ) with Ph_2PCl, have been structurally characterized and the intermediate formation of the diphosphine $Ph_2PN{=}CN(PPh_2)CH_2CH_2S$ (2) has been demonstrated experimentally and by DFT calculations; 2 reacts with [AuCl(THT)] to give [$(AuCl)_2$2] whereas the bidentate metalloligand *cis*-[$Pt(1_{-H})_2$] reacts with AgOTf to form the Ag–Pt coordination polymer $[Ag_\infty[Pt(1_{-H})_2]_\infty](OTf)_\infty$.

The functionalization of phosphine ligands represents a major way to fine-tune their stereoelectronic characteristics and coordination properties as well as the dynamic behaviour and reactivity (stoichiometric and catalytic) of their metal complexes.[1] Increasing the diversity of chemical functions present on such ligands provides considerable opportunities for studying selectivity-related problems. We have now found that when 2-amino-2-thiazoline (ATHZ) is reacted with Ph_2PCl in a 1 : 1 molar ratio, with the original aim of preparing the monophosphine ligand $Ph_2PNHC{=}NCH_2CH_2S$ (**1a**), corresponding to the most stable tautomer of ATHZ,[2] it is in fact the diphosphine $Ph_2PN{=}CN(PPh_2)CH_2CH_2S$ (**2**) that is isolated in almost quantitative yield (based on phosphorus). This is rather surprising in view of recent results obtained with a closely related system.[3] However, when this reaction was performed in the presence of a base like Et_3N or *n*-BuLi, **1** was isolated in two tautomeric forms, **1a** (favoured in non-polar solvents) and **1b**, and **2** was found to be a reaction intermediate (Scheme 1). It will be shown below that the role of the base is to scavenge the HCl liberated in preference to ATHZ. Another intermediate was formed prior to **2** and identified as **3** (as confirmed by ^{31}P NMR when reacting, at low temperature, Ph_2PCl with lithiated ATHZ in large excess, see Supplementary Information), which results from nucleophilic attack of the endo-nitrogen atom of ATHZ on Ph_2PCl. This kinetic product (+19.6 kJ/mol with respect to **1a**), the formation of which is consistent with the endo-nitrogen atom being more nucleophilic than the exo-nitrogen,[4] was found to slowly and quantitatively isomerize to **1**. DFT studies§ suggest for this 1,3-PPh_2 migration an intramolecular mechanism in which the PPh_2 group is transferred from the endocyclic to the exocyclic nitrogen *via* transition state **TS1** (Fig. 1a). Attempts to identify an intermolecular Ph_2P transfer were unsuccessful. The high energy computed for **TS1** (+126 kJ/mol) disfavours this reaction path. In fact, when Ph_2PCl is reacted with ATHZ in a 1 : 1 stoichiometry, an alternative path is preferred. The exocyclic nitrogen of **3**, being more nucleophilic than the endo-nitrogen of ATHZ, rapidly attacks Ph_2PCl, to form **2**. Isolated **2** was shown independently to react with ATHZ to give first **1a**, which rapidly equilibrates with **1b**. Calculations showed that the reaction [**2** + ATHZ → 2 **1a**] is energetically favoured by 6.1 kJ/mol (Fig. 1b). We suggest a concerted mechanism in which the Ph_2P group is transferred from the endocyclic nitrogen of **2** to the exocyclic nitrogen of the ATHZ imino-tautomer while a proton transfer occurs in the opposite direction (Fig. 1b). The calculated transition state **TS2** is

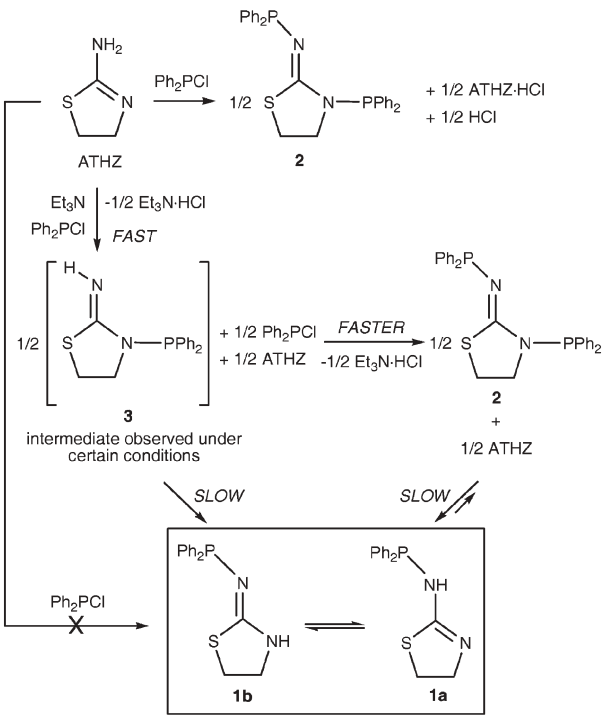

Scheme 1

Laboratoire de Chimie de Coordination, Université Louis Pasteur (UMR 7177 CNRS), Institut Le Bel, 4 rue Blaise Pascal, F-67070, Strasbourg, France. E-mail: braunst@chimie.u-strasbg.fr; Fax: +33390241322; Tel: +33390241308

† Dedicated to Prof. A. Tiripicchio (Parma) on the occasion of his 70th birthday, with our warmest wishes.

‡ Electronic supplementary information (ESI) available: Computed atomic coordinates and distances; complete sets of crystallographic parameters; experimental procedures and spectroscopic characterizations. See DOI: 10.1039/b603495k

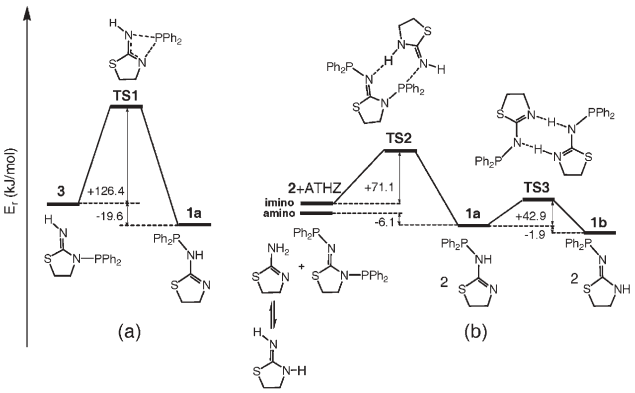

Fig. 1 Relative energy profiles for the intramolecular **1** → **3** tautomerism (a) and the intermolecular ATHZ + **2** → 2 **1** conversion (b).

+71.1 kJ/mol with respect to the reagents (ESI). Summarizing, two pathways are available to form **1**: the aforementioned (disfavoured) direct 1,3-PPh_2 migration in **3** and the reaction of the rapidly formed **2** with the ATHZ present in the reaction mixture (Scheme 1). From the combined theoretical and experimental data, we conclude that the two step conversion **3** → **2** → **1** is preferred to the one step isomerization **3** → **1**. The latter slowly occurs only if Ph_2PCl is unavailable in the reaction mixture, which then precludes the intermediate formation of **2**.

Alternative transition states for the ATHZ + **2** → 2 **1** reaction were computed (ESI). For instance, the conversion featuring the amino-tautomer of ATHZ was found to be energetically disfavoured (+181 kJ/mol), while an activated complex formed by two molecules of ATHZ and one of **2** was calculated to be energetically similar to **TS2** but is entropically disfavoured.

Diphosphine **2** was isolated as the major product when ATHZ was reacted with Ph_2PCl in a 3 : 2 ratio, formation of ATHZ·HCl preventing reaction of the free amine with **2** to give **1**. The molecular structures of **1** and **2**¶ have been determined by X-ray diffraction (Fig. 2).

Tautomers **1a** and **1b** co-crystallized and adopt a head to tail intermolecular arrangement, forming pseudo-dimers through two N···H–N hydrogen bonds. Tautomer **1b** was computed to be only slightly more stable (0.95 kJ/mol) than **1a** and this is consistent with the *ca.* 1 : 1 mixture observed in the solid state. The

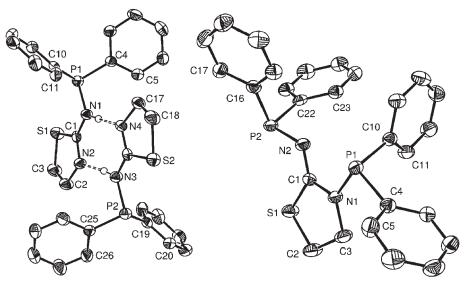

Fig. 2 ORTEP views of the molecular structures of compounds **1** (left) and **2** (right). Displacement parameters include 50% of the electron density. For **1** only one of the two tautomers (**1a**) is shown. Owing to crystallographic disorder, the bond parameters for this ligand are discussed in the Supplementary material. Bond distances (Å) and angles (°) for **2**: S(1)–C(1) 1.7796(17), P(1)–N(1) 1.7511(15), P(2)–N(2) 1.7105(15), N(1)–C(1) 1.364(2), N(2)–C(1) 1.280(2); C(1)–N(1)–C(3) 115.53(14), C(1)–N(1)–P(1) 115.13(12), C(3)–N(1)–P(1) 129.32(12), C(1)–N(2)–P(2) 119.99(12).

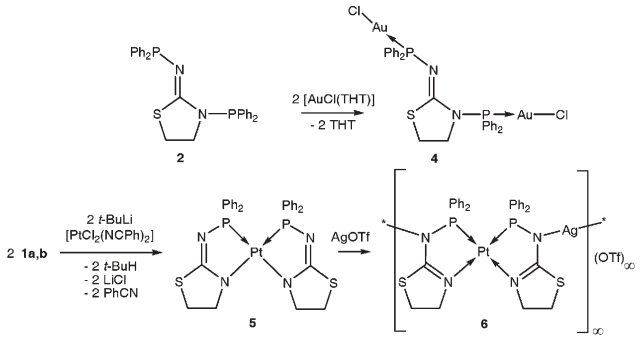

Scheme 2

tautomerism should occur *via* a head to tail transition state (**TS3**). Although phosphine transamination represents a widely used strategy for aminophosphine synthesis (*e.g.* $P(NR_2)_3$, R = Me, Et as starting reagent), only a few examples concerning diaryl- or dialkyl-aminophosphines have been reported.[5] It is remarkable that ATHZ plays a dual role, both as a substrate for Ph_2PCl attack and as a transamination reagent. To the best of our knowledge, this kind of reactivity has never been reported in P(III) chemistry. The P1–N1 bond distance in **2** is significantly longer than P2–N2, consistent with the easier breaking of the endocyclic P–N bond. As expected, the C=N double bond is localized between C1 and the exocyclic N2 atom.

When **2** was reacted with two equivalents of [AuCl(THT)] in CH_2Cl_2, the dinuclear gold complex **4** was formed in quantitative yield (Scheme 2). A view of its molecular structure‖ is shown in Fig. 3.

Each metal centre is coordinated, in a slightly distorted linear geometry, by a chlorine and a phosphorus atom. The coordinated ligand retains a geometry similar to that found in **2**. On the other hand, both P–N distances shorten upon coordination. Reactions of **2** with $[PtCl_2(NCMe)_2]$ or $[PdCl_2(COD)]$ led to the formation of poorly soluble precipitates, which are likely to be oligomeric

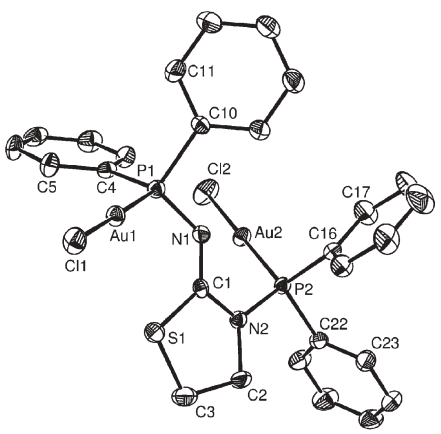

Fig. 3 ORTEP view of the crystal structure of compound **4** in **4**·$CHCl_3$. Displacement parameters include 50% of the electron density. Selected bond distances (Å) and angles (°): Au(1)–P(1) 2.229(2), Au(2)–P(2) 2.2212(17), Au(2)–Cl(2) 2.2834(19), Au(1)–Cl(1) 2.299(2), P(1)–N(1) 1.675(6), P(2)–N(2) 1.713(6), N(2)–C(1) 1.379(8), N(1)–C(1) 1.294(8); P(1)–Au(1)–Cl(1) 174.99(7), P(2)–Au(2)–Cl(2) 177.44(7), N(1)–P(1)–Au(1) 117.2(2), N(2)–P(2)–Au(2) 113.4(2), C(1)–N(1)–P(1) 124.8(5), C(1)–N(2)–P(2) 117.7(4), C(1)–N(2)–C(2) 115.1(5), C(2)–N(2)–P(2) 126.3(5), N(1)–C(1)–S(1) 128.7(5), N(2)–C(1)–S(1) 111.2(5), N(1)–C(1)–N(2) 120.1(6).

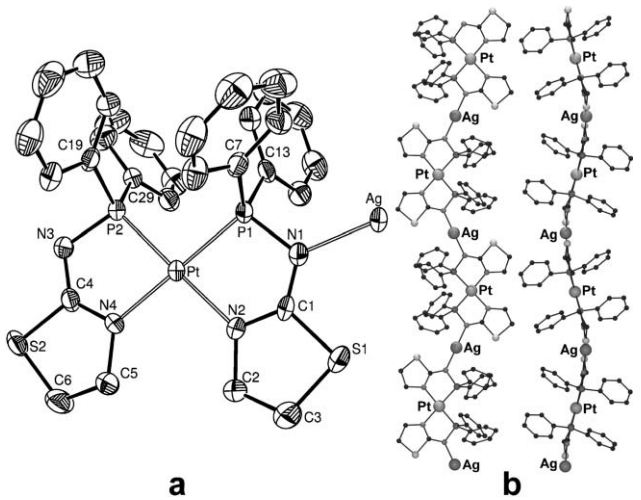

Fig. 4 Views of the crystal structure of compound **6** in **6**·3CH_2Cl_2. Solvent molecules and OTf anions have been omitted for clarity. a) Asymmetric unit (displacement parameters include 50% of the electron density); b) two orthogonal projections of the polymer chain. Selected bond distances (Å) and angles (°): Pt–N(4) 2.084(4), Pt–N(2) 2.096(4), Pt–P(2) 2.2309(14), Pt–P(1) 2.2314(14), Ag(1)–N(3) 2.078(4), Ag(1)–N(1) 2.096(5), P(1)–N(1) 1.686(5), P(2)–N(3) 1.687(5), N(1)–C(1) 1.324(7), N(2)–C(1) 1.307(7), N(4)–C(4) 1.319(7), N(3)–C(4) 1.339(7); N(4)–Pt–N(2) 100.04(18), N(4)–Pt–P(2) 80.95(13), N(2)–Pt–P(1) 80.49(13), P(2)–Pt–P(1) 98.51(5), N(3)–Ag–N(1) 172.08(19).

coordination compounds in which the diphosphine **2** would act as a bridging ligand.

Ligand **1** reacted with *t*-BuLi and [$PtCl_2$(NCPh)$_2$] in a 2 : 2 : 1 ratio to afford the bidentate metalloligand *cis*-[Pt(**1**$_{-H}$)$_2$] (**5**) which, upon reaction with AgOTf, yielded quantitatively the new bimetallic, cationic coordination polymer [Ag_∞[Pt(**1**$_{-H}$)$_2$]$_\infty$](OTf)$_\infty$ (**6**, Scheme 2). Views of the molecular structure of **6**·3CH_2Cl_2** are depicted in Fig. 4.

The platinum coordination geometry is square planar, the four L–Pt–L angles summing to 359.9(2)°, while the Ag atoms, which are bound to the exocyclic N atoms of **5**, adopt a slightly bent geometry [N3–Ag–N1 172.08(19)°]. The C=N double bonds are delocalized over the N1,C1,N2 and N3,C4,N4 atoms, respectively, the C–N distances ranging from 1.307(7) [N2–C1] to 1.339(7) Å [N3–C4].

The resulting infinite chains form a zig-zag and wave-like arrangement (Fig. 4b); the silver atoms occupy the maximum and the minimum points of the sinusoid, and are separated by 9.899(3) Å. To the best of our knowledge, only two examples of structurally characterized Pt–Ag coordination polymers in which linear Ag centres connect Pt metalloligands have been reported before.[6]

The full characterization of tautomers **1a,b** and the intermediate formation of the diphosphine ligand **2** in the course of their synthesis emphasize the subtlety of the bonding in these systems and are relevant to their use in coordination chemistry where ligand interactions with one or many metal centres may profoundly affect the nature of the reactive sites. Further studies with Cu(I), Ag(I) and Au(I) are in progress to delineate the conditions for the formation of new bimetallic coordination polymers.

We thank the Centre National de la Recherche Scientifique, the Ministère de la Recherche, the French Embassy in Berlin and the European Commission (COST D-17 Action) for support. We are grateful to Prof. R. Welter and Dr A. DeCian (ULP Strasbourg) for the crystal structure deteminations and to Prof. P. Hofmann and Dr P. Deglmann (Heidelberg) for access to computing facilities.

Notes and references

§ All calculations were done using the program system TURBOMOLE.[8a] If not mentioned explicitly otherwise, we used the DFT method with the Becke–Perdew functional (BP86).[8b] The Coulomb terms were treated by the RI-J approximation.[8c] For the structure optimizations we used SV(P) basis sets[8d] (single zeta for core orbitals, double zeta for the valence shells and one set of polarization functions for all centres except hydrogen). Single point energies were calculated with larger triple zeta valence plus polarization basis sets (TZVP).[8e]

¶ *Crystal data for* **1**: $C_{15}H_{15}N_2PS$, M = 286.32, monoclinic $P2_1/c$, a = 15.5330(3), b = 11.8340(2), c = 16.1740(3) Å, β = 105.3850(3)°, V = 2866.52(9) Å^3, Z = 8, D_c = 1.327 g cm^{-3}, μ(Mo-Kα) = 0.325 mm^{-1}, F(000) = 1200. A Nonius Kappa CCD diffractometer was employed for the collection of 8350 unique reflections (Mo-Kα, λ = 0.71073 Å, T = 173 K). The structure was solved by direct methods and refined by a full matrix least-squares technique based on F^2 (SHELX97[7]). The final R_1 and wR_2 are 0.046 and 0.112, respectively, for 359 parameters and 5517 reflections [$I > 2\sigma(I)$]. CCDC 601675. The same data collection and refinement procedures were used for **2**, **4**·$CHCl_3$ and **6**·3CH_2Cl_2. *Crystal data for* **2**: $C_{27}H_{24}N_2P_2S$, M = 470.48, triclinic P-1, a = 9.1420(2), b = 10.0760(2), c = 14.4330(4) Å, α = 92.1400(9), β = 105.8700(9), γ = 107.9900(12)°, V = 1205.47(5) Å^3, Z = 2, D_c = 1.296 g cm^{-3}, μ(Mo-Kα) = 0.285 mm^{-1}, F(000) = 492. R_1 and wR_2 are 0.048 and 0.123, respectively, for 289 parameters and 4950 reflections [$I > 2\sigma(I)$] (7015 unique). CCDC 601676. For crystallographic data in CIF or other electronic format see DOI: 10.1039/b603495k

‖ *Crystal data for* **4**·$CHCl_3$: $C_{27}H_{24}Au_2Cl_2N_2P_2S$·$CHCl_3$, M = 1054.68, triclinic P-1, a = 9.610(1), b = 13.281(2), c = 13.769(2) Å, α = 98.04(5), β = 101.87(5), γ = 104.52(5)°, V = 1630.5(4) Å^3, Z = 2, D_c = 2.148 g cm^{-3}, μ(Mo-Kα) = 9.582 mm^{-1}, F(000) = 992. The final R_1 and wR_2 are 0.041 and 0.11, respectively, for 361 parameters and 7031 reflections [$I > 2\sigma(I)$] (9536 unique). CCDC 601677. For crystallographic data in CIF or other electronic format see DOI: 10.1039/b603495k

** *Crystal data for* **6**·3CH_2Cl_2: $C_{30}H_{28}AgN_4P_2PtS$·3CH_2Cl_2·CF_3O_3S, M = 1277.43, monoclinic $P2_1/n$, a = 9.185(3), b = 19.488(6), c = 25.892(9) Å, β = 99.74(2)°, V = 4568(3) Å^3, Z = 4, D_c = 1.858 g cm^{-3}, μ(Mo-Kα) = 4.097 mm^{-1}, F(000) = 2488. R_1 and wR_2 are 0.050 and 0.112, respectively, for 514 parameters and 10225 reflections [$I > 2\sigma(I)$] (13265 unique). CCDC 601678. For crystallographic data in CIF or other electronic format see DOI: 10.1039/b603495k

1 See *e.g.* (*a*) P. Braunstein, *Chem. Rev.*, 2006, **106**, 134; (*b*) P. Braunstein and F. Naud, *Angew. Chem., Int. Ed.*, 2001, **40**, 680; (*c*) G. Helmchen and A. Pfaltz, *Acc. Chem. Res.*, 2000, **33**, 336; (*d*) C. S. Slone, D. A. Weinberger and C. A. Mirkin, *Prog. Inorg. Chem.*, 1999, **48**, 233.
2 Y. Xue, C. K. Kim, Y. Guo, D. Q. Xie and G. S. Yan, *J. Comput. Chem.*, 2005, **10**, 994.
3 H. L. Milton, M. V. Wheatley, A. M. Z. Slawin and J. D. Woollins, *Inorg. Chim. Acta*, 2005, **358**, 1393.
4 (*a*) M. Avalos, R. Babiano, P. Cintas, M. M. Chavero, F. J. Higes, J. L. Jimenez, J. C. Palacios and G. Silvero, *J. Org. Chem.*, 2000, **65**, 8882; (*b*) G. Kaugars, S. E. Martin, S. J. Nelson and W. Watt, *Heterocycles*, 1994, **12**, 2593.
5 (*a*) N. V. Dubrovina, V. I. Tararov, Z. Kadyrova, A. Monsees and A. Boerner, *Synthesis*, 2004, **12**, 2047; (*b*) E. V. Bakhmutova, H. Nöth, R. Contreras and B. Wrackmeyer, *Z. Anorg. Allg. Chem.*, 2001, **627**, 1846; (*c*) V. L. Foss, Y. A. Veits, T. E. Chernykh and I. F. Lutsenko, *Zh. Obshch. Khim.*, 1984, **54**, 2670.
6 (*a*) P. Strickler, *Helv. Chim. Acta*, 1969, **52**, 270; (*b*) I. B. Rother, M. Willermann and B. Lippert, *Supramol. Chem.*, 2002, **14**, 189.
7 G. M. Sheldrick, *SHELX-97*, University of Göttingen: Germany, 1997.
8 (*a*) R. Ahlrichs, M. Bär, M. Häser, H. Horn and C. Kölmel, *Chem. Phys. Lett.*, 1989, **162**, 165; (*b*) A. D. Becke, *Phys. Rev. A*, 1988, **38**, 3098; (*c*) K. Eichkorn, O. Treutler, H. Ohm, M. Häser and R. Ahlrichs, *Chem. Phys. Lett.*, 1995, **240**, 283; (*d*) A. Schäfer, H. Horn and R. Ahlrichs, *J. Chem. Phys.*, 1992, **97**, 2571; (*e*) A. Schäfer, C. Huber and R. Ahlrichs, *J. Chem. Phys.*, 1994, **100**, 5829.

